Determination of forming limits of TWIP steel sheet using linear and nonlinear strain paths

P Farahnak, M Urbanek, M Rund and J Dzugan

COMTES FHT a.s., Prumyslova 995, 334 41 Dobrany, Czech Republic

Corresponding author's E-mail: pedram.farahnak@comtesfht.cz

Abstract. The main goal of the present paper is investigation of the mechanical behaviour of high manganese content steel sheet which is well known in the literature as Twinning-Induced Plasticity (TWIP) under linear and nonlinear loading path. Contrary to Nakajima experiment, cruciform specimen under biaxial loading can provide linear and nonlinear strain path. This work aims to determine the numerical Forming Limit Curve (FLC) for TWIP sheet using cruciform specimen under biaxial loading. For this purpose, uniaxial tensile tests are performed on standard dog-bone samples which are extracted from rolling, transversal and diagonal directions to identify the flow curve as well as Lankford ratios. Data are used as input for numerical simulation of cruciform specimen. Results show the applicability of cruciform specimen for linear and nonlinear strain paths.

1 Introduction

The Forming Limit Diagram (FLD) introduced by Keeler [1], has been used extensively in sheet metal forming. Forming Limit Curve (FLC) is a plot of the major and minor principal strains in the plane of deformed sheet where necking takes place. The Nakajima experiment is often adopted as the conventional experiment for FLC determination. Thus, different samples with a variety of widths have to be tested in order to cover whole FLC from the uniaxial to equi-biaxial strain range. However, in this experiment contact between the punch and sheet influences the real formability of the material. As reported in the literature [2], the main challenge is to experience a pure biaxial mode and predictions are difficult as a consequence. Contact condition can be in the form of either pressure or friction [3, 4]. Friction can cause variation and the test has to be repeated while punch pressure on sheet leads to overestimation of the material formability [5].

The biaxially loaded cruciform specimen was designed as an alternative for the Nakajima test as a friction-free test. The original sheet thickness of the investigated TWIP steel is $1.5\ mm$ in the present work. Based on a special design of cruciform specimen, necking is induced by groove construction in the central region. The influence of thickness on material formability and fracture were investigated in [6-8]. In the central region, the geometry has thickness variation from minimum $0.3\ mm$ to maximum $1.5\ mm$. Afterwards, the displacement ratio of the actuators can control the strain path in the region.

TWIP steel is known for its combination of very high strength with extreme elongation capacity. This steel was selected for shock tower apron reinforcement. Chemical composition is summarized in table 1. In this work, uniaxial samples were extracted from sheet in Rolling, Transverse and Diagonal

Content from this work may be used under the terms of the Creative Commons Attribution 3.0 licence. Any further distribution of this work must maintain attribution to the author(s) and the title of the work, journal citation and DOI.
Published under licence by IOP Publishing Ltd

Directions and are denoted by (RD), (TD) and (DD), respectively. Afterwards, uniaxial test were done on samples. Flow curve and Lankford ratios were characterized by using Digital Image Correlation (DIC) system. These data are used as input for numerical simulation of cruciform specimen under linear and nonlinear loading conditions. The experimental setup and details will be explained in section 2.

Table 1. Chemical composition of TWIP steel

C [%]	Mn [%]	P [%]	S [%]	Cr [%]
0.068	4.96	0.009	0.004	0.049

2 Material characterization

Figure 1 depicts the geometry of standard dog-bone specimen. For characterization of Lankford ratios, samples are extracted from the experimental sheet in the Rolling, Diagonal and Transverse Directions and values are denoted by r_0, r_{45} and r_{90}, respectively. Electro-mechanical testing system, Mayes, is used to conduct the uniaxial tests and the GOM Aramis™ system with a 12 megapixel camera is utilized to monitor $2D$ strain fields with high resolution. The data acquisition rate is set at $100\ Hz$ in the testing system for accurate measuring of the tensile behaviour. It is noticed that for the standard dog-bone geometry, initial length of extensometers is chosen as $80\ mm$. Figure 2(a) represents the engineering stress-strain curves of tensile tests for rolling, transverse and diagonal directions. The Abaqus FEM base software is utilized for numerical simulation with conventional plasticity [9] based on von Mises material. Flow curve in figure 2(b), is extrapolated using linear combination of Voce-Swift (equation (2)) and parameter γ in equation (3), is calibrated through inverse analysis by comparing numerical and experimental force-displacement curves (figure 2(c)) and parameters are summarized in table 2. Mesh sizes in the centre of specimen was $0.8\ mm$ and in surrounding area was $1.2\ mm$.with 4 C3D8R elements (according to Abaqus library) along the thickness.

Gauge sections are defined in transversal direction as well. Three experiments are performed on the specimens in rolling, diagonal and transversal directions. GOM Aramis™ captures 2D displacement fields during deformation, e.g., axial and transversal extensometers with facet size of $16\ pixels$ provide engineering surface strains and these are then transformed into true values. Finally, thickness strain is measured based on the incompressibility condition. The Lankford ratio can be calculated from the average slope of true plastic width (ε_w^p) and thickness (ε_{th}^p) strain in equation (1) in a specific range of equivalent plastic strain ($0.1 \leq \bar{\varepsilon}_p \leq 0.2$) and values are depicted in Figure 2 (d).

$$r = \frac{d\varepsilon_w^p}{d\varepsilon_{th}^p} \tag{1}$$

$$K_{Voce} = k_0 + Q\left(1 - \exp\left(-\beta\bar{\varepsilon}_p\right)\right) \tag{2}$$

$$K_{Swift} = A(\varepsilon_0 + \bar{\varepsilon}_p)^n$$

$$\bar{\sigma}_p = \gamma K_{Swift} + (1-\gamma)K_{Voce} \tag{3}$$

3 Cruciform specimen

One of the ways how to achieve experimentally a linear and nonlinear strain path is the biaxial test. Biaxial testing machines can depict the real behavior of materials without effect of the friction [10]. Moreover, for linear and nonlinear strain paths measurement, cruciform specimen can be utilized without friction. The main difficulty of the cruciform specimen is necking imposition in the central region of the specimen due to thickness reduction or thinner gauge. If necking is induced to the central region, then the loading ratios of the machine can control the strain paths in the center of gauge. In

previous work s[11], the cruciform geometry was optimized for biaxial test, using FEM simulations in order to achieve maximum deformation in the central region and not in the shoulders. The optimized

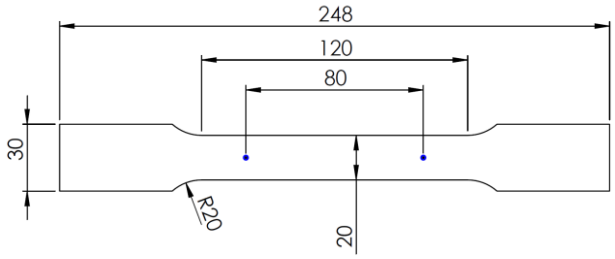


Figure 1. Geometry of dog-bone specimen

Table 2. Voce- Swift flow curve parameters

Voce			Swift			Linear combination
k_0 [MPa]	Q [MPa]	β	A [MPa]	ε_0	n	γ
410	900	6	2400	0.2	0.9	0.08

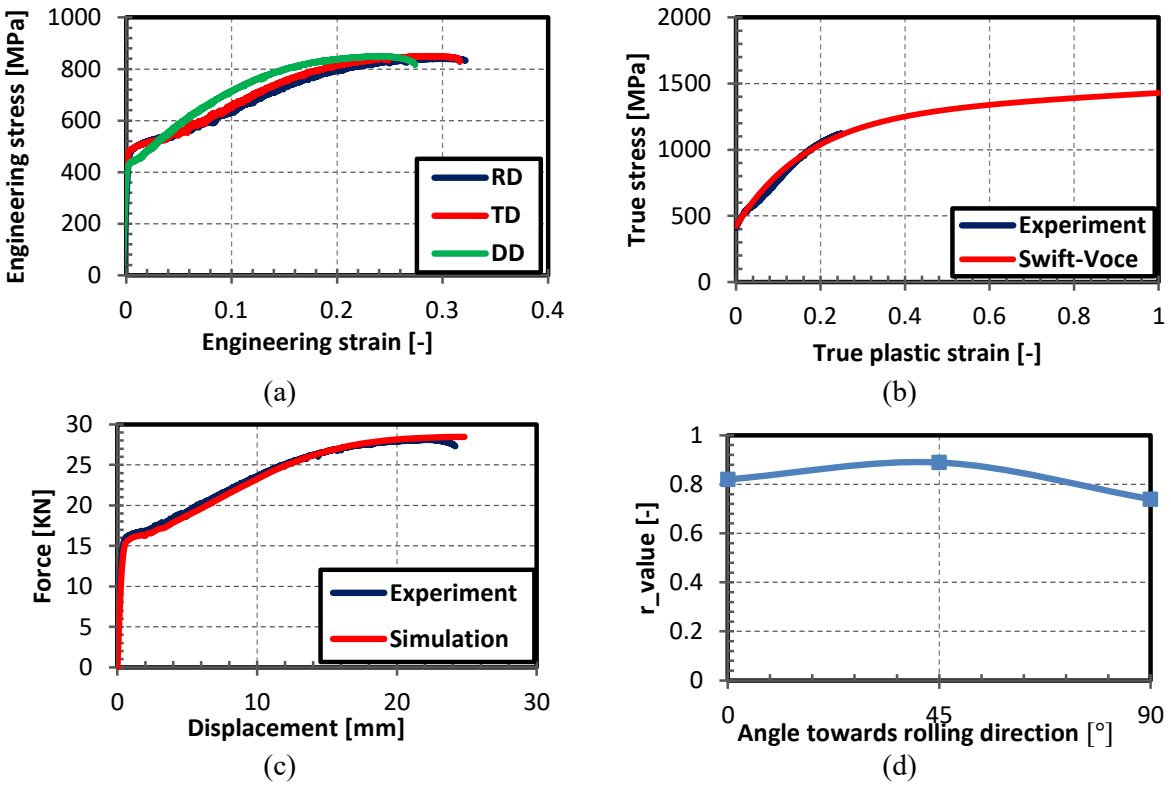


Figure 2. (a) Engineering stress-strain curves in different orientation (b) Extrapolated flow curve (c) Experimental and numerical force-displacement curves (d) Lankford ratios

gauge is similar to cruciform specimen [12], but the thickness ratios are different. The thickness of the thinner gauge is 0.3 mm. Geometry of the cruciform with thickness variations is depicted figure 3.

3.1 Numerical simulation of the cruciform specimen

Plasticity parameters from Section 2 are used as input for FEM simulation of cruciform specimen with the thickness variation to clarify how material characterization based on medium and small specimens can influence the strain path. The aim of numerical simulation is to represent the real-world

experiment as accurately as possible. Theory of Hill 48 and the influence of anisotropy parameters on strain path was investigated by Farahnak et al [13].

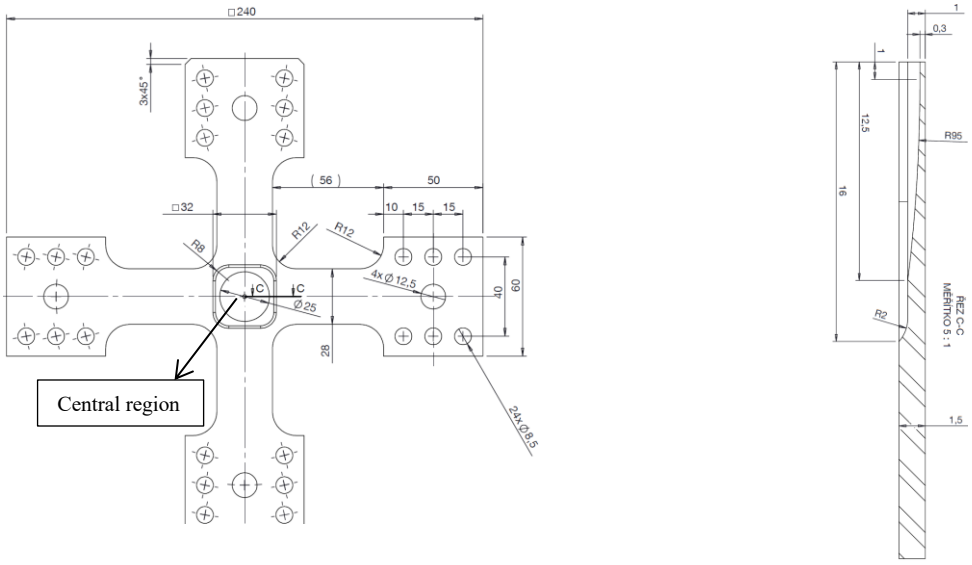


Figure 3. Geometry of cruciform specimen with longitudinal thickness variations

Mesh size plays a prominent role in numerical simulation of cruciform specimen, e.g. with a coarse mesh necking can take place in higher level of strains and subsequently it can affect the strain path's slope and necking. Therefore, for all simulations, one quarter of the cruciform geometry is modelled using 0.8 mm mesh size in the central region , 1 mm for surrounding areas and 6 elements along the thickness with $3D$ elements with 8 nodes (C3D8 according to Abaqus). A mesh size smaller than these values leads to time-consuming calculation and does not have significant influence on the results. In all simulations, strain paths are plotted for central elements where the deformation is maximum.

For linear strain paths, major strains are plotted in terms of minor strains for uniaxial, plane strain and equi-biaxial loading conditions and are indicated in figure 4(a). Beginning time of instability is detected using the first and second derivation method in the thinnest element [14] and as an example for equi-biaxial loading condition is depicted in figure 4(b). As can be seen in the figure, peaks are rigorously localized in terms of simulation time.

For nonlinear strain paths, combinations of equi-biaxial tension-plane strain tension and uniaxial tension-equi-biaxial tension are taken into account in the present paper and strain paths are shown in figure 4(c) and (d), respectively. As can be seen in figure 4(c) and (d), different numerical steps are highlighted with different colors. It is noticeable that for both nonlinear strain paths, force imposed on RD. Take equi-biaxial tension-plane strain tension experiment as an example, the experiment is started under equi-biaxial tension with force imposition in RD and TD and then for plane strain tension, cruciform specimen in TD is clamped for numerical simulation. Therefore, RD was subjected to main deformation during numerical simulations.

Besides, stress triaxiality (λ) and equivalent plastic strain ($\bar{\varepsilon}_p$) as ductile damage parameters are plotted in the center of cruciform specimen and shown in figure 5. Stress triaxiality can be defined as the ratio of hydrostatic pressure to the equivalent stress and its values corresponding to uniaxial, plane strain and equi-biaxial tensions are summarized in table 3 as follow:

Table 3. Stress triaxiality values in different loading conditions

Loading condition	Uniaxial	Plane strain	Equi-biaxial
λ	0.33	0.57	0.66

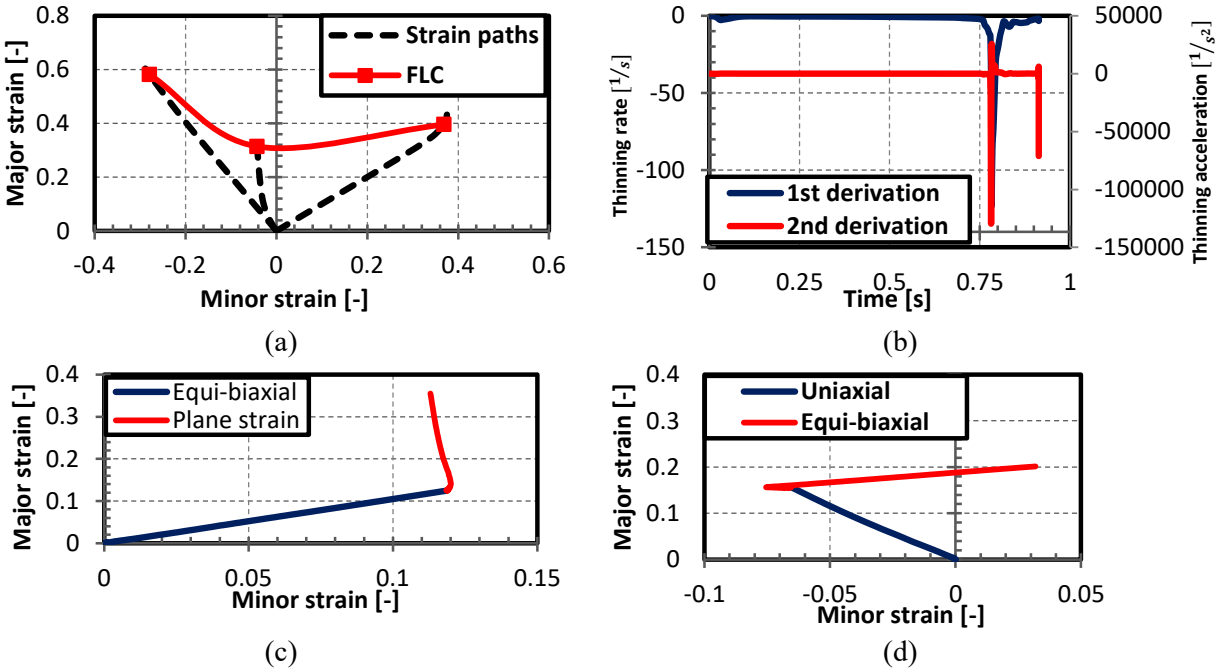


Figure 4. (a) Numerical FLC (b) Example of derivation method for necking detection (c) Nonlinear strain path, equi-biaxial tension- plane strain tension (d) Nonlinear strain path, uniaxial tension - equi-biaxial tension

It is obvious in figure 5 how the stress triaxiality changes by changing the loading condition. In figure 5(a), after changing the loading condition from equi-biaxial tension to plane strain tension, there is an evolution for stress triaxiality to attain the ideal value in table 3. However, there is a discrepancy in figure 5(b) between numerical and ideals values for stress triaxiality, which is most common for cruciform specimens during uniaxial tensile tests. As can be seen in the figure, after changing the loading condition from uniaxial tension to equi-biaxial tension, stress triaxiality almost attains 0.66 corresponding to equi-biaxial loading condition.

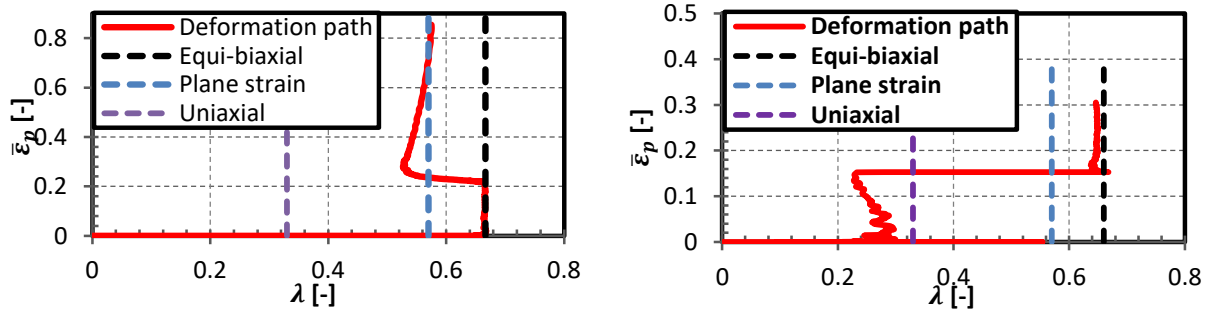


Figure 5. Nonlinear deformation paths (a) Equi-biaxial tension- plane strain tension (b) Uniaxial tension- equi-biaxial tension

4 Conclusion

This work introduce cruciform specimen as an alternative for Nakajima experiment since it can provide frictionless FLC from uniaxial tension to equi-biaxial tension. In addition, it can provide nonlinear and complex loading paths. The cruciform geometry was optimized in previous works and the idea was as follows: If necking is induced to the central region, then the loading ratios of the machine can control the strain paths in the center of gauge. Therefore, uniaxial tensile test in different material directions were performed. Flow curve and Lankford ratios were characterized for TWIP steel

sheet. Those parameters were used as input for numerical simulation of the cruciform specimen with using Hill 48 anisotropic yield criterion. First and second derivation methods were utilized to detect the beginning time of instability. Peaks in first and second derivations are rigorously localized in terms of time. Therefore, a numerical FLC was presented for the material under investigation. Cruciform specimen was simulated under nonlinear loading paths as well. In the present work, equi-biaxial tension- plane strain tension and uniaxial tension- equi-biaxial tension were taken into account. Deformation paths in terms of strain and stress triaxiality were plotted. It was shown how stress triaxiality changes by changing the loading condition. This work only investigates the plastic behavior of a TWIP steel sheet considering anisotropic effects. Extensions to fracture as well as experiments are deferred to future research.

Acknowledgements
This paper is a result of the project "Methods development for formability assessment of thin sheets considering anisotropy and non-linear loading path" No.: TF02000072, financed by Technology Agency of the Czech Republic.

References

[1] Keeler S and Backofen W 1963 *J. Transaction of American society for metals,* Plastic instability and fracture in sheets stretched over rigid punches, **56** 25-48.
[2] Lester S, Nikhare C 2014 *International Deep Drawing Research Group (IDDRG),* Investigation of strain development and hole expansion ratio in mild steel and AA5083, 210-15
[3] Kuwabara T, Hashimoto K, Iizuka E and Yoon J 2014 *J. Mater. Process. Technol* Effect of anisotropic yield functions on the accuracy of forming simulations of hole expansion **81** 2433-38.
[4] Ram S and Kang H 2010 *ASME International Mechanical Engineering Congress and Exposition,* Investigation of hole expansion characteristics of DP 600 with testing and modelling **3** 47-51.
[5] Nikhare C, Vorisek E, Nolan J and Roth J 2017 *Journal of Engineering Materials and Technolgy* Forming limit differences in hemispherical dome and biaxial test during equibiaxial tension on cruciform **139** 0410111-9.
[6] Farahnak P, Urbanek M, Konopik P and Dzugan J 2018, *Int J Mater Form,* Determination of formability limits of mild steel DC01 using Nakajima and cruciform experiments with consideration of thickness influence on strain path (under submission).
[7] Urbanek M, Farahnak P, Rund M and Dzugan J 2018, *Journal of physics,* Sheet thickness reduction influence on fracture strain determination, **1063**.
[8] Konopik P, Farahnak P, Rund M, Prochazka R and Dzugan J 2018,*Ubiquity Proceedings,* Application of micro-tensile test for material characterization of mild steel DC01, DOI: https://doi.org/10.5334/uproc.33
[9] Farahnak P, Azinpour E, Belinha J and sa J 2016 The numerical non-linear analysis of elasto-plastic materials using the radial point interpolation method *International book of Material Modelling: Applications, Challenges and Research* 215-248 ISBN: 978-1-53612-161-2.
[10] AbuFarha F, Hector L and Kharisheh M 2009 *Met. Mater, Soc. (TMS),* Cruciform-shaped specimen for elevated temperature biaxial testing for lightweight materials, **61**(8) pp.48-56.
[11] Prantl A, Urbanek M, Prochazka R and Dzugan J 2016 *International Deep Drawing Research Group (IDDRG),* Evaluation of influence of strain path on FLD diagram.
[12] Zidane I, Guines D, Leotoing L and Ragneau E 2010 *Measurement Science and Technology* Development of an in-plane biaxial test for forming limit curve (FLC) characterization of metallic sheets, **21,** 1-11.
[13] Farahnak P, Dzugan J and Prantl A 2016 *International conference of COMAT,* **179** 012023. Sheet necking prediction in forming limit diagrams with the anisotropy influence incorporation
[14] Farahnak P, Dzugan J and Urbanek M 2017 *International conference of Deep Drawing Research Group* **896** 012082. Investigation study on determination of fracture strain and fracture forming limit curve using different experimental and numerical methods